IEEE Access
Multidisciplinary | Rapid Review | Open Access Journal

Received 20 July 2023, accepted 3 August 2023, date of publication 9 August 2023, date of current version 15 August 2023.

Digital Object Identifier 10.1109/ACCESS.2023.3303812

RESEARCH ARTICLE

Modeling the Dispersion and Nonlinearity of the Hollow ZBLAN Microfiber in the Mid-Infrared Region

WEI SHU, LIMING DING, (Member, IEEE), AND XIANWU MI
School of Physics, Electronics and Intelligent Manufacturing, Huaihua University, Huaihua 418000, China
Key Laboratory of Intelligent Control Technology for Waling-Mountain Ecological Agriculture in Hunan Province, Huaihua 418000, China
Corresponding author: Liming Ding (shuwei@hhtc.edu.cn)

ABSTRACT ZBLAN fiber is widely used in the mid-infrared band, mainly for spectrum, sensing, laser power transmission, fiber laser, and amplifier. By tapering the soft glass optical fiber such as ZBLAN fiber to microfiber, the waveguide behavior can be tailored in the mid-IR spectral range to realize large normal waveguide dispersion. However, the tunability of the dispersion and nonlinearity must be further explored. Because hollow waveguides offer various compelling features, we proposed and designed a hollow ZBLAN microfiber to adjust the dispersion and nonlinearity and numerically investigated the fundamental propagation characteristics of hollow ZBLAN microfibers within the 2–5 μm mid-infrared spectral range. The three-layer-dielectric circular waveguide structure was modeled, and the waveguide dispersion, group velocity dispersion, and nonlinearity coefficients of hollow ZBLAN microfibers were investigated. The numerical results showed that the hollow ZBLAN microfiber exhibits broadband dispersion compensation and tunable nonlinear coefficient when its geometry is tailored. The proposed method can be used to manipulate the propagation characteristics of the microfiber in the mid-infrared regime, and the results provide a reference for the design of high-performance mid-infrared optoelectronic devices.

INDEX TERMS Hollow waveguides, mid-infrared band, nonlinear optics, optical fiber dispersion, ZBLAN.

I. INTRODUCTION

Low-loss, dispersion, and nonlinearity tunable fiber components that operate in the mid-infrared (mid-IR) spectral range are highly required in versatile applications in spectroscopy, medicine, military, remote sensing, and material processing [1]. In recent years, with the rapid development of optical fiber systems, researchers have investigated and developed near-infrared and mid-IR wavelength optical fiber and optical-fiber-based equipment suitable for various applications [2], [3], [4]. Among the low-loss mid-IR optical materials, ZBLAN glass has a wide transparent window that extends from the deep-ultraviolet (200 nm) to the mid-IR (8 μm) regime [5], [6]. The intrinsic material loss for ZBLAN is less than 0.01 dB/km at the 2.5-μm mid-IR wavelength region, which suggests the possibility of shifting the communication wavelength to a longer wavelength with much lower loss [7]. As the most common composition of heavy metal fluoride glass, ZBLAN glass is the ideal candidate to make optical fiber due to its most stable characteristics in fluoride glasses [8]. Until now, the ZBLAN fiber has been widely used in infrared bands mainly for sensing, laser power transmission, amplifier, fiber laser, and nonlinear optics [9], [10], [11].

Generating a supercontinuum (SC) spectrum in the infrared band is one of the most important applications of ZBLAN fiber. A large-range SC spectrum that extends to the mid-IR has been produced in ZBLAN fiber, which has been widely reported recently [12], [13], [14]. As we all know, the generation of an SC spectrum is a combination of the dispersion effect and various nonlinear optical effects. The fiber dispersion and nonlinear characteristics can be tailored by varying its geometry to modify the waveguide dispersion [15]. The basic characteristics of the uniform hexagonal lattice ZBLAN photonic crystal fiber (PCF) are numerically

The associate editor coordinating the review of this manuscript and approving it for publication was Yang Yue.

studied, such as the normalized frequency, limited loss, dispersion, effective mode area, and nonlinear coefficient, providing a reference for the design of ZBLAN PCF with different functions within the 2–3 μm mid-IR wavelength region [16], [17]. The optical properties of tapered ZBLAN (such as the dispersion, nonlinearity, and confinement loss for the fundamental mode (FM)) delayed Raman response, and material losses were investigated to generate SC in a tapered fiber structure [13].

For other typical applications, ZBLAN fibers can be used as a dispersion compensator. Unlike the near-infrared regime, the conventional optical fibers in the mid-IR regime usually exhibit anomalous dispersion. However, normal dispersion is highly required for dispersion compensation in high-energy pulse generation and pulse compression. Although the dispersion compensation can be realized through free-space grating compressors, the configuration will make the system bulky and complicated. A waveguide with specific dispersion and nonlinearity can be designed and realized via microstructured optical fiber, with which the dispersion, effective mode area, and nonlinear coefficient can be manipulated. However, the complicated preparation procedures will limit the applications of the microstructured optical fiber. Another simple method to tune the dispersion and nonlinearity is to taper it. By tapering soft glass optical fiber such as ZBLAN fiber to microfiber, the waveguide behavior can be tailored in the mid-IR spectral range to realize large normal waveguide dispersion [18]. However, the tunability of the dispersion and nonlinearity must be further explored.

Hollow waveguides have attracted extensive attention in the field of photonics since the concept of infrared hollow fiber was proposed, and they have been widely used in optical communication, optical sensing, nonlinear optics, and other fields [19], [20], [21]. Compared with standard silica fiber, hollow fiber has a delay reduction of approximately 30%, a higher damage threshold, and a lower nonlinear response by more than three orders of magnitude, which is very beneficial for satisfying the emerging capacity and delay requirements in future optical network [22], [23]. Compared with silica (SiO_2) hollow nanowires [24], [25] and $LiNbO_3$ hollow nanowires [26], ZBLAN hollow nanowires can manipulate waveguide performance within the mid-IR wavelength region.

A series of reports has been proposed to fabricate hollow fibers with different internal structures. In 2002, Fitt et al. used asymptotic analysis to propose leading-order equations for the drawing of a capillary, and the process is considered the first step toward a complete quantification of the process of drawing arbitrarily shaped holey fibers [27]. Kolyadin et al. discussed the optical transmission of negative curvature hollow fibers, whose core diameter is 119 μm, and the capillary wall thickness is 6 μm [28]. Kosolapov et al. reported the fabrication of the first hollow-core revolver fiber with a core diameter as small as 25 mm and low loss at a wavelength of 1850 nm [29]. Jung et al. fabricated several example HCF components with low insertion loss, low Fresnel reflection, and high modal purity using various state-of-the-art HCFs [30]. Fabricating high-quality microfibers is complex. Yaman et al. reported a new thermal size-reduction process to produce well-ordered, globally oriented, indefinitely long nanowire and nanotube arrays with different materials, where the nanowire diameters were less than 15 nm [31]. With constant technological advances, hollow microfiber fiber can be produced with high yields and repeatability.

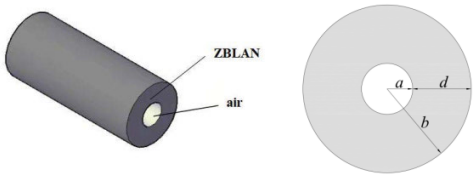

FIGURE 1. Schematic of the hollow ZBLAN microfiber: structure and dimension parameters.

Here, we have numerically investigated the basic propagation characteristics of hollow ZBLAN microfibers. By modeling the waveguide with a three-layer-dielectric circular waveguide structure, the effective index, waveguide dispersion, group velocity dispersion, and nonlinearity coefficients of hollow ZBLAN microfibers have been investigated. The numerical results show that the hollow ZBLAN microfiber exhibits broadband dispersion compensation and a tunable nonlinear coefficient by tailoring the geometry of the hollow ZBLAN microfiber. Our simulation results predict that by adjusting the waveguide design parameters, we can achieve a low dispersion of 17–24 ps·nm^{-1}·km^{-1} over a bandwidth of 2500 nm. The structure shows a high dispersion value of -6022.78 ps·nm^{-1}·km^{-1} at 2.85 μm. This study should be useful for the application of SC generation and the design of dispersion compensation structures.

II. THEORETICAL MODEL

Fig. 1 shows the schematic of the hollow ZBLAN microfiber and radius of each area of the cross section. The hollow ZBLAN microfiber has a three-layer cylindrical dielectric structure with rotational symmetry. We assume that the hollow ZBLAN microfiber is isotropic, piecewise homogeneous, and infinitely long on the z-axis.

The refractive indices of the air -core n_s and outer infinite air cladding n_c are 1.0. The ZBLAN fiber has the component 55.8ZrF_4-14.4BaF_2-5.8LaF_3-3.8AlF_3-20.2NaF, and the refractive indices of the core for ZBLAN can be obtained using the following Sellmeier functions [18]:

$$n_f^2(\lambda) = 1 + \frac{1.168\lambda^2}{\lambda^2 - 0.0954^2} + \frac{2.77\lambda^2}{\lambda^2 - 25^2} \tag{1}$$

During the numerical calculation, we only consider the FMs of the hollow ZBLAN microfiber. The transverse field components are obtained based on the Helmholtz equation in the homogeneous sections when the refractive index is

constant [32], [33].

$$\left[\frac{1}{\mathrm{r}}\frac{\partial}{\partial r}\left(r\frac{\partial}{\partial r}\right)+\frac{1}{\mathrm{r}^2}\frac{\partial^2}{\partial\varphi^2}\left(k_0^2n^2-\beta^2\right)\right]\begin{pmatrix}E_z\\H_z\end{pmatrix}=0 \quad (2)$$

where k_0 is the free-space wave number; Ez and Hz are the z components of the field.

All transverse components, including E_r, $E_\emptyset$, H_r, and $H_\emptyset$, can be easily obtained through the relevant formula related to E_z and H_z.

Applying boundary conditions at $r = a$ and $r = b$, we obtain the matrix equation after lengthy rearrangements of eight linear homogeneous equations. The propagation constant β can be solved when the determinant of the linear equations is zero:

$$\det\left[M\left(\beta\right)\right]=0 \quad (3)$$

where M is the resulting matrix of the system of equations.

Then, the group velocities (V_g) and waveguide dispersions (D_w) are easily obtained using the following equations [34]:

$$V_g=\frac{d\omega}{d\beta}=-\frac{2\pi c}{\lambda^2}\frac{d\lambda}{d\beta} \quad (4)$$

$$D_w=\frac{d\left(V_g^{-1}\right)}{d\lambda} \quad (5)$$

The group velocity dispersion (GVD) parameter β_2 is

$$\beta_2=-\frac{\lambda^2D_w}{2\pi c} \quad (6)$$

The confinement loss (CL) can be calculated using the following formula [35]:

$$CL=\frac{40\pi}{\ln(10)\lambda}\mathrm{Im}(n_{eff})=8.868k_0\mathrm{Im}(n_{eff}) \quad (7)$$

in decibels per meter, where $\mathrm{Im}(n_{eff})$ is the imaginary part of the complex effective refractive index.

Finally, the nonlinear coefficient γ is obtained [28]

$$\gamma=\frac{2\pi}{\lambda}\frac{\int n_2S_z^2d^2r}{\left(\int S_zd^2r\right)^2} \quad (8)$$

Here, $n_2 = 5.4 \times 10^{-16}$ cm^2/W is the nonlinear refractive index of refraction for ZBLAN [16]. Compared with that of ZBLAN, we assume that n_2 of air is negligible in our calculations; S_z is the longitudinal component of the Poynting vector, which can be obtained through numerical calculation according to the field distribution. We have set the initial phase to be $\varphi_1 = 0$.

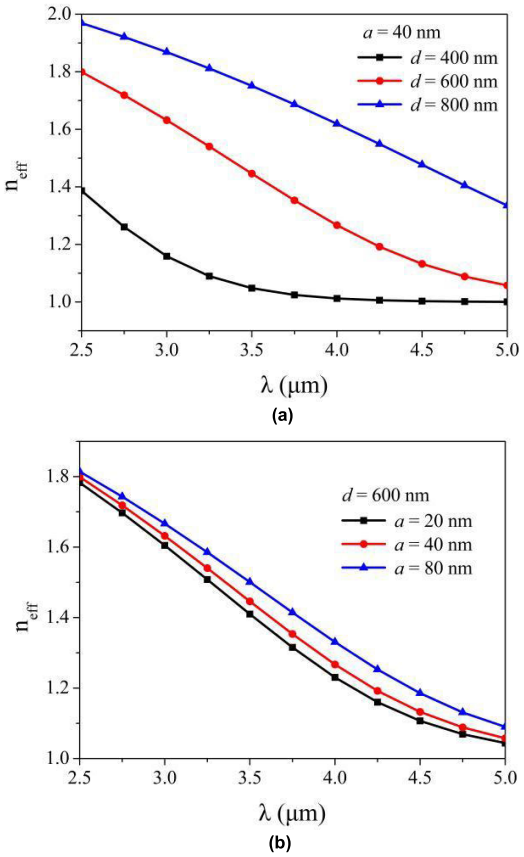

FIGURE 2. Effective index curves of the fundamental mode for hollow ZBLAN microfiber. (a) Air-core radius α = 40 nm with different thicknesses d of the ZBLAN region; (b) ZBLAN region thickness d = 600 nm with different air-core radii α.

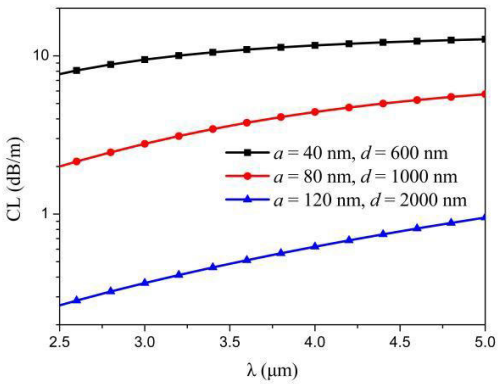

FIGURE 3. Confinement loss curves for hollow ZBLAN microfiber with different air-core radii and ZBLAN region thicknesses.

III. RESULTS AND DISCUSSION

A. MODAL CHARACTERISTICS

The modal properties of the hollow ZBLAN microfiber are analyzed using numerical simulation within the wavelength range of 2.5–5 μm in this section.

By sweeping the wavelength, we can obtain the effective index of the FM as a function of the wavelength. When the air-core was assumed to be 40 nm and the ZBLAN region thicknesses d varied from 400 nm to 800 nm, Fig. 2(a) shows the effective index curve of the FM for the hollow ZBLAN microfiber. As shown in Fig. 2(b), when the ZBLAN region thickness d was assumed to be 600 nm and the air-core radius a increased from 20 nm to 80 nm, the effective index curve of FM reduced accordingly. Numerical calculations show that the effective refractive index increases with the size of the hollow fiber and decreases with the wavelength.

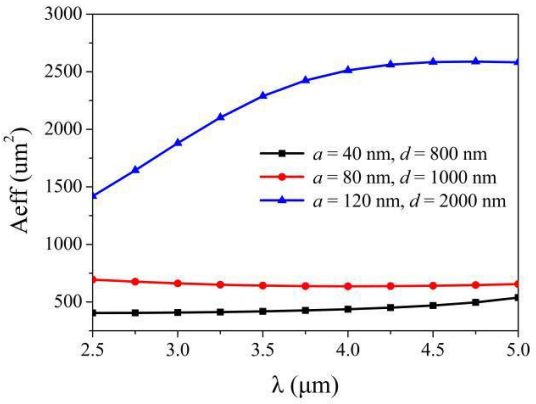

FIGURE 4. Effective mode area curves of the fundamental mode for hollow ZBLAN microfiber with different air-core radii α. ZBLAN region thickness d = 600 nm.

Fig. 3 shows the confinement loss as a function of the wavelength with different air-core a and ZBLAN region thicknesses d.

The confinement loss is 0.28 dB/m for $a = 120$ nm, $d = 2000$ nm and reaches 8.09 dB/m for $a = 40$ nm, $d = 600$ nm at 2.6 μm. The confinement losses significantly increase with decreasing diameter of the hollow ZBLAN microfiber. The main reason is that the effective index of the ZBLAN region increases with a larger thickness, which results in a larger effective index difference between the microfiber core and air cladding.

We calculated the effective mode area A_{eff} of several hollow ZBLAN microfibers with different sizes, and Fig. 4 shows the results. The nonlinear effect decreases with the increase in A_{eff}; the nonlinear effect of the hollow ZBLAN microfiber can be adjusted by changing the air-core radius and ZBLAN region thickness.

The power density distribution in optical fiber can clearly explain the field distribution, which is very important in waveguide design. The thickness of the hollow microfiber and high contrast between the refractive indices of the ZBLAN and the air-core will substantially modify the intensity distributions. Fig. 5(a–f) shows the profiles of the power density of the hollow ZBLAN microfiber with an evanescent field by gradient profile when $a = 40$ nm, $d = 600$ nm and $a = 120$ nm, $d = 2000$ nm at 2.52 μm, 3.3 μm, and 4.1 μm. All evanescent waves are guided inside the hollow ZBLAN microfiber. Attributed to the electric field discontinuity at the boundary between the air-core and dielectric region, the intensity in the central hollow region has been enhanced when the diameter of the hollow ZBLAN microfiber increases. Fig. 5(a–f) demonstrates that the power density value decreases when the wavelength increases.

B. WAVEGUIDE DISPERSION

The fiber dispersion can be tailored by varying its geometry to modify the waveguide dispersion [15]. ZBLAN has quite favorable material dispersion performance with a zero dispersion wavelength (ZDW) approaching 1.6 μm and a relatively flat dispersion profile, which requires only a mild waveguide contribution to the total dispersion to form a second ZDW at a longer wavelength [13].

Fig. 6 shows the dispersion curves of the hollow ZBLAN microfiber with various air-core radii, where the ZBLAN region thickness is $d = 400$ nm. As shown in the figure, the air-core radius is $a = 10$ nm, the ZDW is approximately 2.19 μm, and the dispersion maximum is -6022.78 ps·nm^{-1}·km^{-1} at 2.85 μm. Then, when the wavelength increases, the dispersion value decreases, and the dispersion value is -35.77 ps·nm^{-1}·km^{-1} at 5 μm. When the air-core radius increases to 80 nm, the ZDW shifts to approximately 2.52 μm, and the dispersion maximum is -4567.29 ps· nm^{-1}· km^{-1} at 3.3 μm. Both normal dispersion and abnormal dispersion regions were obtained. When the air-core radius of the hollow ZBLAN microfiber increases, the dispersion maximum point and ZDW shift toward long wavelengths, and the maximum dispersion value decreases.

The dispersion value is related to the changes in wavelength and effective refractive index. Compared with the largest value of -478.3 ps· nm^{-1}· km^{-1} achieved at 3.0 μm for ZBLAN PCF [16], the maximum dispersion increases by more than 10 times. Hollow ZBLAN microfibers obtain larger dispersion values than photonic crystal fibers.

With varying ZBLAN region thicknesses, the dispersion curves change. The dispersion is numerically calculated when the air-core size is designed to be 10 nm. For comparison, the ZBLAN region thicknesses are set to 400 nm, 600 nm, 800 nm, and 1000 nm. Fig. 7 shows the waveguide dispersion curves with various ZBLAN region thicknesses. The ZDW shifts to 4.37 μm when the ZBLAN region thickness d increases to 800 nm and disappears in the 2–5 μm wavelength range when the ZBLAN region thickness d increases to 1000 nm. When the air-core radius is $a = 10$ nm and the ZBLAN region thickness is $d = 1000$ nm, all dispersion values are positive, and the numerical range is 80–600 ps·nm^{-1}·km^{-1}. In past research, the ZDW of the ZBLAN microfiber is approximately 1.49 μm [9]. By changing the air-core radius and ZBLAN region thickness, the ZDW successfully shifts to the mid-IR band. Compared with changing the air-core radius, changing the thickness of the ZBLAN region more significantly affects the dispersion.

According to the sign of the dispersion parameter, the nonlinear effect in the optical fiber shows significantly different characteristics. With the disappearance of ZDW, we continued to study the change in dispersion with increasing air-core radius and ZBLAN region thickness. Fig. 8 shows the waveguide dispersion curves with different thicknesses d of the ZBLAN region when air-core radius $a = 400$ nm. With the increase in thickness of the ZBLAN region, the waveguide dispersion value is positive, and the curve changes are increasingly smooth. Fig. 8 also shows that when the ZBLAN region thickness is greater than 2000 nm, the dispersion values are positive, and the dispersion values are 60–80 ps·nm^{-1}·km^{-1}.

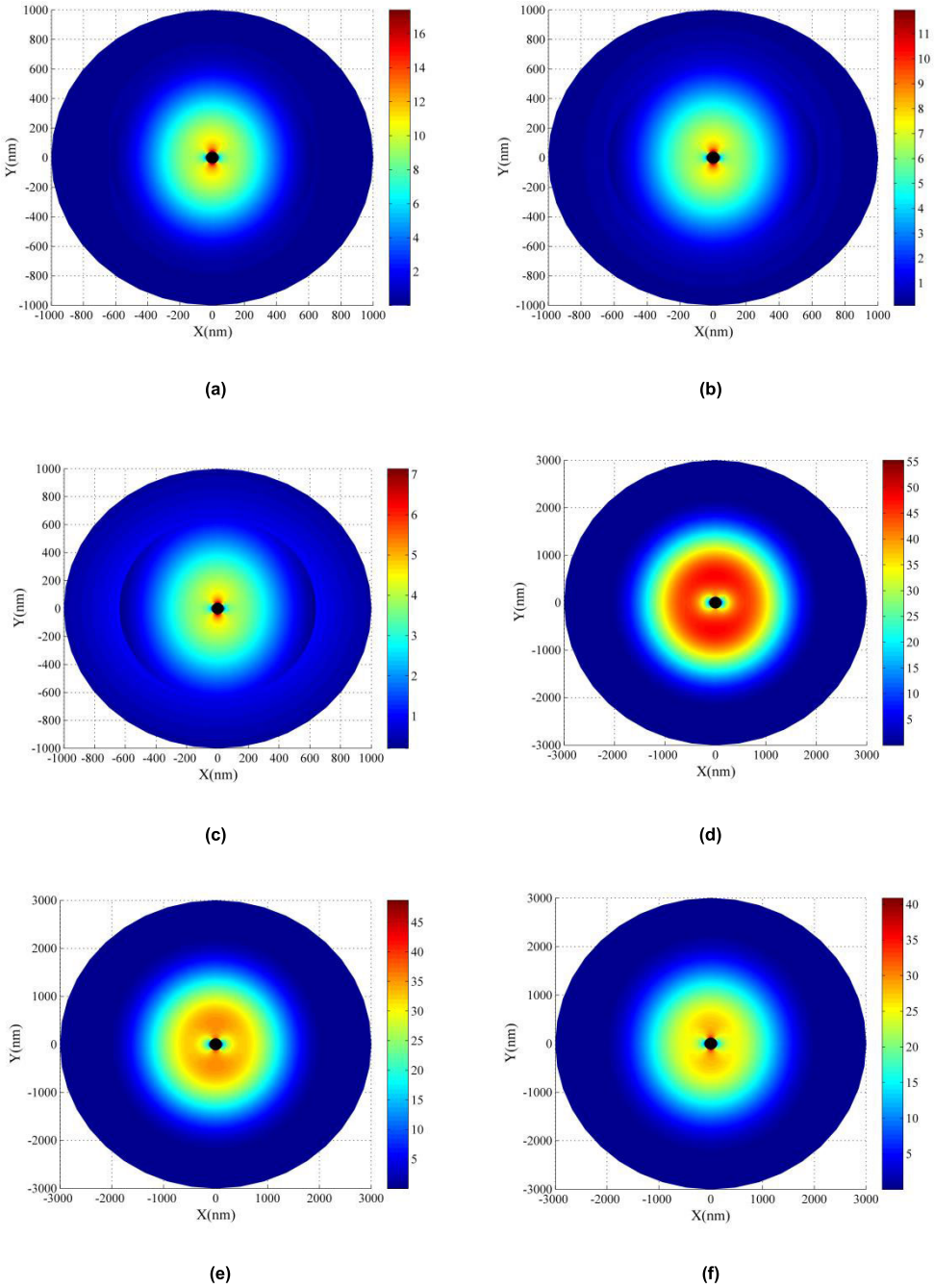

FIGURE 5. Profile of the power density of the hollow ZBLAN microfiber with a fundamental mode state. (a) α = 40 nm, d = 600 nm, λ =2.52 μm; (b) α = 40 nm, d = 600 nm, λ =3.3 μm; (c) α = 40 nm, d = 600 nm, λ =4.1 μm; (d) α = 120 nm, d = 2000 nm, λ =2.52 μm; (e) α = 120 nm, d = 2000 nm, λ =3.3 μm; (f) α = 120 nm, d = 2000 nm, λ = 4.1 μm.

To further investigate the significant changes in dispersion values of the ZBLAN region thickness from 1000 nm to 2000 nm, we studied the dispersion value when the ZBLAN region thickness was 1500 nm, as shown in Fig. 9. Fig. 9 shows that the change in dispersion value is basically linear despite different air-core radii. Moreover, the dispersion value has a small variation range in the mid-IR band; the change in dispersion value is the smallest especially when the air-core size is 400 nm. When the hollow size increases to 800 nm, the dispersion value appears negative with the increase in wavelength, and the ZDW appears at approximately 4.54 μm.

By changing the structural parameters of the hollow ZBLAN microfiber, the dispersion characteristics are controllable. According to the required dispersion value and dispersion variation range, the numerical results provide a reference for the design of waveguide structures and optical devices.

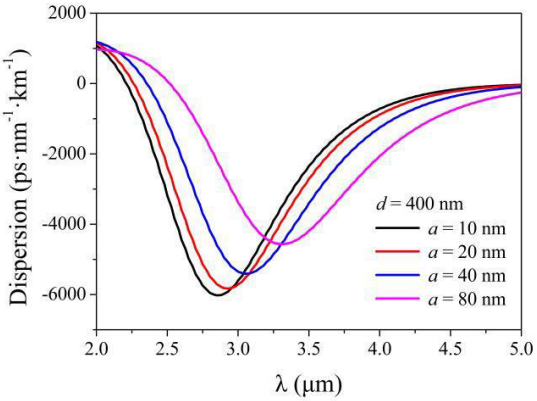

FIGURE 6. Dispersion curves of the hollow ZBLAN microfiber for ZBLAN region thickness d = 400 nm with different air-core radii.

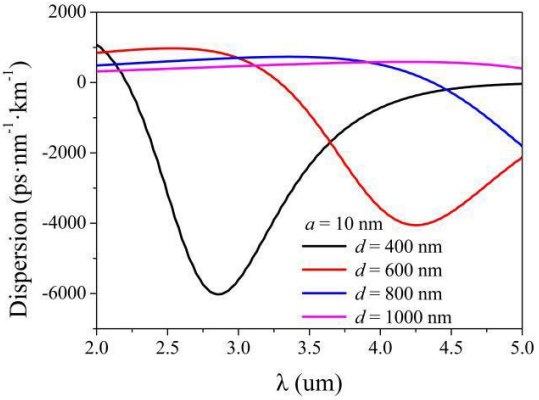

FIGURE 7. Dispersion curves of the hollow ZBLAN microfiber for air-core radius α = 10 nm with different ZBLAN region thicknesses d.

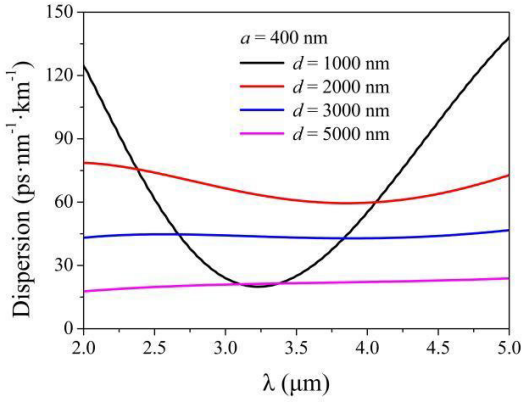

FIGURE 8. Dispersion curves of the hollow ZBLAN microfiber with different thicknesses d of the ZBLAN region. Air-core radius α = 400 nm.

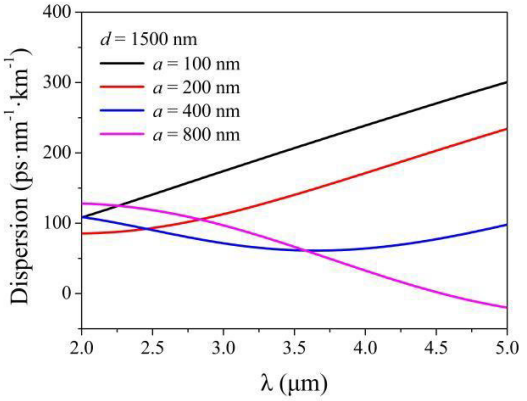

FIGURE 9. Dispersion curves of the hollow ZBLAN microfiber with different air-core radii α. ZBLAN region thickness d = 1500 nm.

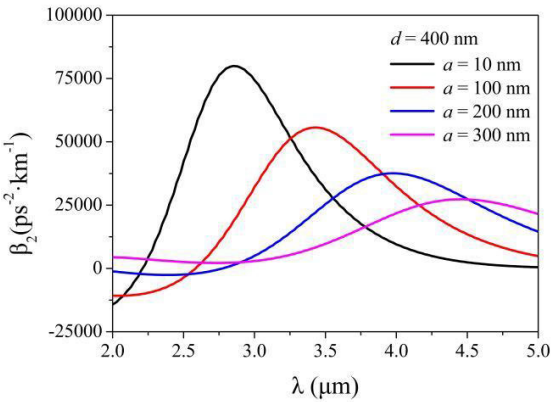

FIGURE 10. GVD characteristics of the hollow ZBLAN microfiber with different ZBLAN air-core radii α. ZBLAN region thickness d = 400 nm.

C. GVD PARAMETER

Due to the normal dispersion of ZBLAN fiber, the application as a dispersion compensator has been widely studied. ZBLAN microfiber has large normal dispersion for the wavelength range of 2–5 μm by tailoring the fiber geometry [36]. Fig. 10 shows the GVD characteristics of the hollow ZBLAN microfiber with different air-core radii within the 2–5 μm mid-IR wavelength region. The result shows that large normal dispersion of the hollow ZBLAN microfiber can be obtained by decreasing the fiber air-core size. With the increase in the air-core size, the maximum value of GVD decreases and moves to the long wavelength, and the change in numerical value is more gentle. The GVD parameter can be easily adjusted by varying the hollow ZBLAN microfiber air-core size. To clarify the potential dispersion compensating ability of the hollow ZBLAN microfiber, the GVD of the hollow ZBLAN microfiber with different ZBLAN region thicknesses has been discussed, as shown in Fig. 11. Similar to the effect of an increasing air-core radius, the maximum value of GVD decreases, and the maximum point moves to the long wavelength with the increase in ZBLAN region thickness. The broadband GVD can be obtained by tailoring the geometry of the hollow ZBLAN microfiber, which is significant in optical communication and nonlinear optics.

D. NONLINEAR COEFFICIENT

The highly non-linear, dispersion flattened fiber plays a central role in the generation of an ultra-wide and high-power SC. Fig. 12 shows the nonlinear coefficients γ for various core radii with the change in wavelength when ZBLAN region thickness d = 400 nm. The hollow ZBLAN microfiber exhibits a high nonlinear coefficient at the wavelength range of 2–3 μm. The nonlinear coefficient γ = 399.79 W^{-1}/km has been achieved in the optimized hollow ZBLAN microfiber with air-core radius a = 10 nm

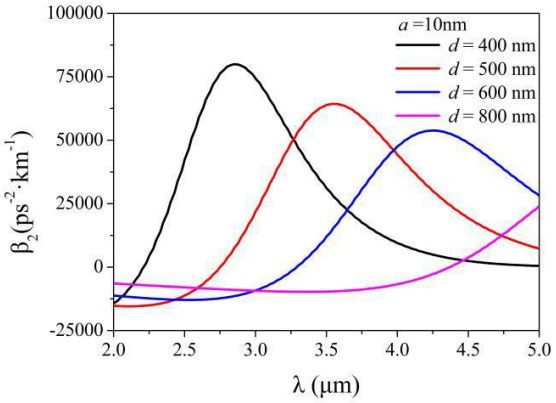

FIGURE 11. GVD characteristics of the hollow ZBLAN microfiber with different ZBLAN region thicknesses d. Air-core radius α = 10 nm.

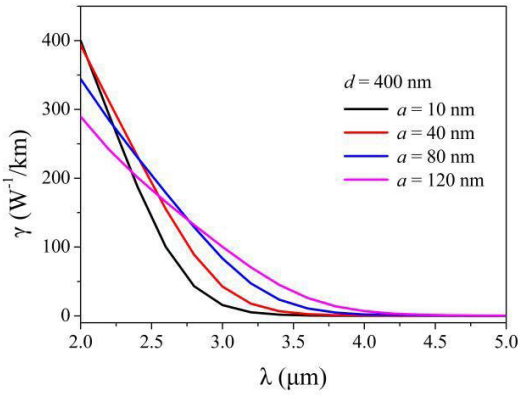

FIGURE 12. Nonlinear coefficient of the hollow ZBLAN microfiber for the ZBLAN region thickness d = 400 nm.

and ZBLAN region thickness d = 400 nm at the pumping wavelength of 2 μm. Fig. 12 shows that with the increase in wavelength, the corresponding nonlinearity decreases, and it sharply decreases especially at a wavelength of 2–4 μm. When the air-core size decreases, the maximum value and value range of the nonlinear coefficient decrease, and the decline becomes slower. The influence of the ZBLAN region thickness d on the nonlinear coefficient is also illustrated. If the air-core size a is 400 nm, Fig. 13 shows the nonlinear coefficient curves with various ZBLAN region thicknesses of hollow microfiber. When the ZBLAN region thickness increases, the effective area increases, and the nonlinear coefficient decreases.

A high nonlinear optical fiber is conducive to the occurrence of nonlinear effects, but for optical communication, a low nonlinear optical fiber is a better choice. Due to the lower nonlinearity of the ZBLAN material, ZBLAN fiber tapering has been studied for the generation of mid-IR coherent continuous spectrum [37], and a ZBLAN PCF with low nonlinear coefficients is designed for communication in 2–3 μm mid-IR [38]. Compared with ZBLAN fiber taper and ZBLAN PCF, the nonlinear coefficient of the small-size hollow microfiber is significantly improved. For the large variation range of the nonlinear coefficient, the hollow ZBLAN

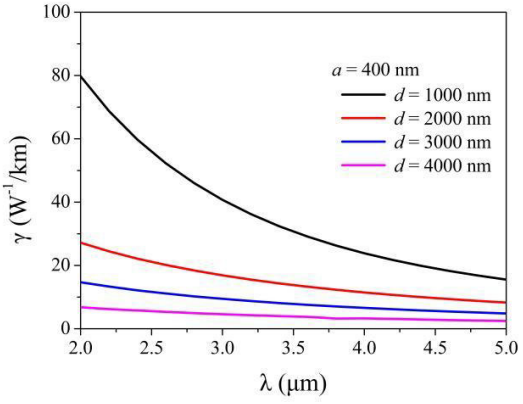

FIGURE 13. Nonlinear coefficient of the hollow ZBLAN microfiber for air-core radius α = 400 nm.

microfiber exhibited an extensive application prospect in nonlinear optics.

IV. CONCLUSION

We investigated the effect of various waveguide design parameters on the propagation characteristics of hollow ZBLAN microfibers in the mid-IR band. By tailoring the waveguide geometry, the ZDW can move to a longer wavelength with the increase in the air-core size and thickness, and the maximum dispersion value also moves to the longer band. When the ZBLAN region thickness increases to 2 μm, the dispersion value is positive and gently changes. The nonlinear coefficient of the hollow ZBLAN microfiber varies by approximately 20 times from 2 to 4 μm wavelength when the ZBLAN region thickness changes from 400 nm to 5 μm. By optimizing the geometric parameters such as the air-core radius and ZBLAN region thickness, the dispersion and nonlinear coefficient can be manipulated to achieve versatile applications. The proposed method can be used to manipulate the propagation characteristics of the microfiber in the mid-IR regime, and the results provide a reference for the design of high-performance mid-IR optoelectronic devices.

REFERENCES

[1] G. Zhu, "Fe^{2+}:ZnSe and graphene Q-switched singly Ho^{3+}-doped ZBLAN fiber lasers at 3 μm," *Opt. Mater. Exp.*, vol. 3, no. 9, pp. 1365–1377, Aug. 2013, doi: 10.1364/ome.3.001365.

[2] S. D. Jackson, "Towards high-power mid-infrared emission from a fibre laser," *Nature Photon.*, vol. 6, no. 7, pp. 423–431, Jun. 2012, doi: 10.1038/nphoton.2012.149.

[3] A. Barh, S. Ghosh, G. P. Agrawal, R. K. Varshney, I. D. Aggarwal, and B. P. Pal, "Design of an efficient mid-IR light source using chalcogenide holey fibers: A numerical study," *J. Opt.*, vol. 15, no. 3, Feb. 2013, Art. no. 035205, doi: 10.1088/2040-8978/15/3/035205.

[4] A. Barh, "An efficient broadband mid-wave IR fiber optic light source: Design and performance simulation," *Opt. Exp.*, vol. 21, no. 8, pp. 9547–9555, 2013, doi: 10.1109/IPCon.2013.6656543.

[5] M. Cable and J. M. Parker, *High-Performance Glasses*. London, U.K.: Chapman & Hall, 1992, pp. 145–147.

[6] J. S. Sanghera and I. D. Aggarwal, *Infrared Fiber Optics*. Boca Raton, FL, USA: CRC Press, 1998, pp. 64–67.

[7] X. Jiang, "Deep-ultraviolet to mid-infrared supercontinuum generated in solid-core ZBLAN photonic crystal fibre," *Nature Photon.*, vol. 9, no. 2, pp. 133–139, 2015, doi: 10.1038/NPHOTON.2014.320.

[8] X. Zhu and N. Peyghambarian, "High-power ZBLAN glass fiber lasers: Review and prospect," *Adv. OptoElectronics*, vol. 2010, pp. 1–23, Mar. 2010, doi: 10.1155/2010/501956.
[9] A. Jin, Z. Wang, J. Hou, B. Zhang, and Z. Jiang, "Experimental measurement and numerical calculation of dispersion of ZBLAN fiber," in *Proc. Int. Conf. Electron. Optoelectron.*, vol. 3, Jul. 2011, pp. V3-181–V3-184, doi: 10.1109/ICEOE.2011.6013332.
[10] C. R. Day, P. W. France, S. F. Carter, M. W. Moore, and J. R. Williams, "Fluoride fibres for optical transmission," *Opt. Quantum Electron.*, vol. 22, no. 3, pp. 259–277, May 1990, doi: 10.1007/BF02189431.
[11] G. Androz, "2.3 W single transverse mode thulium-doped ZBLAN fiber laser at 1480 nm," *Opt. Exp.*, vol. 1, no. 16, pp. 16019–16031, Sep. 2008, doi: 10.1364/OE.16.016019.
[12] C. L. Hagen, J. W. Walewski, and S. T. Sanders, "Generation of a continuum extending to the midinfrared by pumping ZBLAN fiber with an ultrafast 1550-nm source," *IEEE Photon. Technol. Lett.*, vol. 18, no. 1, pp. 91–93, Jan. 2006, doi: 10.1109/LPT.2005.860390.
[13] Z. Chen, A. Taylor, and A. Efimov, "Coherent mid-infrared broadband continuum generation in non-uniform ZBLAN fiber taper," *Opt. Exp.*, vol. 17, no. 7, pp. 5852–5860, Mar. 2009, doi: 10.1364/OE.17.005852.
[14] C. Xia, "10.5 W time-averaged power Mid-IR supercontinuum generation extending beyond 4 μm with direct pulse pattern modulation," *IEEE J. Sel. Topics Quantum Electron.*, vol. 15, no. 2, pp. 422–434, Apr. 2009, doi: 10.1109/JSTQE.2008.2010233.
[15] G. P. Agrawal, *Nonlinear Fiber Optics*, 3rd ed. San Diego, CA, USA: Academic, 2001, pp. 424–426.
[16] Y. Gao, J.-F. Li, Y.-Z. Wang, Y.-W. Shi, F. Liu, K. Li, J. Yang, and Y. Liu, "Design of ultra large normal dispersion ZBLAN photonic crystal fiber and its application in mid-IR ultra short fiber lasers," *IEEE Photon. J.*, vol. 10, no. 6, pp. 1–9, Dec. 2018, doi: 10.1109/JPHOT.2018.2872985.
[17] P. S. Maji and P. R. Chaudhuri, "Design of all-normal dispersion based on multimaterial photonic crystal fiber in IR region for broadband supercontinuum generation," *Appl. Opt.*, vol. 54, no. 13, pp. 4042–4048, Apr. 2015, doi: 10.1364/AO.54.004042.
[18] Q. Yang, L. Miao, G. Jiang, and C. Zhao, "Modeling the broadband mid-infrared dispersion compensator based on ZBLAN microfiber," *IEEE Photon. Technol. Lett.*, vol. 28, no. 7, pp. 728–731, Apr. 1, 2016, doi: 10.1109/LPT.2015.2506646.
[19] T. Hidaka, T. Morikawa, and J. Shimada, "Hollow-core oxide-glass cladding optical fibers for middle-infrared region," *J. Appl. Phys.*, vol. 52, no. 7, pp. 4467–4471, Jul. 1981, doi: 10.1063/1.329373.
[20] L. Jin, B.-O. Guan, and H. Wei, "Sensitivity characteristics of Fabry–Pérot pressure sensors based on hollow-core microstructured fibers," *J. Lightw. Technol.*, vol. 31, no. 15, pp. 2526–2532, Aug. 2013, doi: 10.1109/JLT.2013.2269136.
[21] J. Yu, X. Li, X. Tang, H. Zhang, N. Chi, and Y. Shi, "High-speed signal transmission at W-band over dielectric-coated metallic hollow fiber," *IEEE Trans. Microw. Theory Techn.*, vol. 63, no. 6, pp. 1836–1842, Jun. 2015, doi: 10.1109/TMTT.2015.2425888.
[22] F. Poletti, N. V. Wheeler, M. N. Petrovich, N. Baddela, E. N. Fokoua, J. R. Hayes, D. R. Gray, Z. Li, R. Slavík, and D. J. Richardson, "Towards high-capacity fibre-optic communications at the speed of light in vacuum," *Nature Photon.*, vol. 7, no. 4, pp. 279–284, Mar. 2013, doi: 10.1038/NPHOTON.2013.45.
[23] S. A. Mousavi, "Nonlinear dynamic of picosecond pulse propagation in atmospheric air-filled hollow core fibers," *Opt. Exp.*, vol. 26, no. 7, pp. 8866–8882, Apr. 2018, doi: 10.1364/OE.26.008866.
[24] C. Zhao, "Field and dispersion properties of subwavelength-diameter hollow optical fiber," *Opt. Exp.*, vol. 15, no. 11, pp. 6629–6634, May 2007, doi: 10.1364/OE.15.006629.
[25] H. Xiao-Hong, Z. Wei, G. Yong-Kang, W. Lei-Ran, L. Ke-Qing, and L. Xue-Ming, "Mode field diameter and nonlinear properties of air-core nanowires," *Chin. Phys. B*, vol. 18, no. 8, pp. 3183–3188, Aug. 2009, doi: 10.1088/1674-1056/18/8/015.
[26] H. He, M. Wu, L. Miao, Z. Deng, G. Jiang, J. Luo, C. Zhao, and S. Wen, "Propagation characteristics of anisotropic *a*-axis hollow lithium niobate nanowire," *J. Lightw. Technol.*, vol. 34, no. 17, pp. 4028–4035, Sep. 1, 2016, doi: 10.1109/JLT.2016.2593733.
[27] A. D. Fitt, "The mathematical modelling of capillary drawing for holey fibre manufacture," *J. Eng. Math.*, vol. 43, nos. 2–4, pp. 201–227, 2002, doi: 10.1023/A:1020328606157.
[28] A. Kolyadin, "Light transmission in negative curvature hollow core fiber in extremely high material loss region," *Opt. Exp.*, vol. 21, no. 8, pp. 9514–9519, Apr. 2013, doi: 10.1364/OE.21.009514.
[29] A. F. Kosolapov, G. K. Alagashev, A. N. Kolyadin, A. D. Pryamikov, A. S. Biryukov, I. A. Bufetov, and E. M. Dianov, "Hollow-core revolver fibre with a double-capillary reflective cladding," *Quantum Electron.*, vol. 46, no. 3, pp. 267–270, Mar. 2016, doi: 10.1070/QEL15972.
[30] Y. Jung, "Compact micro-optic based components for hollow core fibers," *Opt. Exp.*, vol. 28, no. 2, pp. 1518–1525, 2020, doi: 10.1364/OE.28.001518.
[31] M. Yaman, T. Khudiyev, E. Ozgur, M. Kanik, O. Aktas, E. O. Ozgur, H. Deniz, E. Korkut, and M. Bayindir, "Arrays of indefinitely long uniform nanowires and nanotubes," *Nature Mater.*, vol. 10, no. 7, pp. 494–501, Jul. 2011.
[32] E. Karadeniz, "Intercore-cladding uniaxial dielectric thin film optical fibers," *Opt. Eng.*, vol. 45, no. 8, Aug. 2006, Art. no. 085001, doi: 10.1117/1.2337644.
[33] U. Schröter and A. Dereux, "Surface plasmon polaritons on metal cylinders with dielectric core," *Phys. Rev. B, Condens. Matter*, vol. 64, no. 12, Sep. 2001, Art. no. 125420, doi: 10.1103/PhysRevB.64.125420.
[34] L. M. Tong, J. Lou, and E. Mazur, "Single-mode guiding properties of subwavelength-diameter silica and silicon wire waveguides," *Opt. Exp.*, vol. 12, no. 6, pp. 1025–1035, Mar. 2004, doi: 10.1364/OPEX.12.001025.
[35] P. S. Maji and P. R. Chaudhuri, "Supercontinuum generation in ultra-flat near zero dispersion PCF with selective liquid infiltration," *Optik*, vol. 125, no. 20, pp. 5986–5992, Oct. 2014, doi: 10.1016/j.ijleo.2014.07.026.
[36] M. A. Foster, K. D. Moll, and A. L. Gaeta, "Optimal waveguides dimensions for nonlinear interactions," *Opt. Ex.*, vol. 12, no. 13, pp. 2880–2887, Jun. 2004, doi: 10.1364/OPEX.12.002880.
[37] I. Kubat, "Mid-infrared supercontinuum generation to 4.5 μm in uniform and tapered ZBLAN step-index fibers by direct pumping at 1064 or 1550 nm," *J. Opt. Soc. Amer. B, Opt. Phys.*, vol. 30, no. 9, pp. 2743–2757, Oct. 2013, doi: 10.1364/JOSAB.30.002743.
[38] D. C. Tee, N. Tamchek, and C. H. R. Ooi, "Numerical modelling of fundamental characteristics of ZBLAN photonic crystal fiber for communication in 2–3 μm mid-infrared region," *IEEE Photon. J.*, vol. 8, no. 2, pp. 1–14, Apr. 2016, doi: 10.1109/JPHOT.2016.2536940.

WEI SHU received the B.S. degree in electronic science and technology from Northwest Polytechnic University, in 2008, and the M.S. degree in information and communication from Hunan University, in 2011. She is currently a Lecturer with Huaihua University. Her current research interests include optical waveguides theory and nonlinear fiber optics.

LIMING DING (Member, IEEE) received the B.S. degree in mathematics and applied mathematics from the Hunan University of Science and Technology, Xiangtan, China, in 2007, the M.S. degree in computer application technology from the Kunming University of Science and Technology, Kunming, China, in 2010, and the Ph.D. degree in control science and engineering from Central South University, Changsha, China, in 2017. He was a Lecturer in teaching and research section for computer with the Department of Public Courses, Hunan University of Medicine, and has been an Associate Professor with the School of Electrical and Information Engineering, Huaihua University, since 2019. His current research interests include time-delay systems and networked control systems.

XIANWU MI was born in Hunan, China. He received the Ph.D. degree in microelectronics and solid state electronics from the Shanghai Institute of Microsystems and Information Technology, Chinese Academy of Sciences, Shanghai, China, in 2006. He is currently with the Key Laboratory of Intelligent Control Technology for Wuling-Mountain Ecological Agriculture in Hunan Province, Huaihua University. His current research interest includes optical sensing and devices in ecological agriculture.